Polymer 53 (2012) 1925–1931

Contents lists available at SciVerse ScienceDirect

Polymer

journal homepage: www.elsevier.com/locate/polymer

Structural relaxation of polystyrene in nanolayer confinement

Deepak S. Langhe [a], Thomas M. Murphy [b], Andrew Shaver [a], Christine LaPorte [a], B.D. Freeman [b], D.R. Paul [b], E. Baer [a,*]

[a] Center for Layered Polymeric Systems, Department of Macromolecular Science and Engineering, Case Western Reserve University, Cleveland, OH 44106-7202, USA
[b] Department of Chemical Engineering, The University of Texas at Austin, Austin, TX 78712, USA

ARTICLE INFO

Article history:
Received 14 November 2011
Received in revised form
18 February 2012
Accepted 24 February 2012
Available online 1 March 2012

Keywords:
Physical aging
Nanolayer confinement
Glassy polymers

ABSTRACT

The physical aging of polystyrene (PS) confined in a multilayered film arrangement was explored using differential scanning calorimetry (DSC). The multilayered films were produced via multilayer coextrusion and consisted of alternating layers of PS and polycarbonate (PC), with PS layer thicknesses ranging from 50 nm to 500 nm. A 125 μm bulk control film of pure PS was also extruded and studied for comparison. The glass transition temperatures (T_g) of the PS in multilayered films did not appear to be systematically dependent on layer thickness, and T_g values in all PS/PC films were similar to the bulk value of 104 °C. Two approaches were used to investigate the structural relaxation of PS in the layered films. In the first method, PS layers were aged isothermally at 80 °C after annealing above the T_g of PS (135 °C for 15 min) to reset the thermal history and provide a well-defined starting point for aging experiments. Recovered enthalpy data for aged films (calculated from DSC thermograms) showed that the aging rate in the PS layers decreased with decreasing layer thickness. Calculated aging rates were also compared with the fraction of interphase material (which increases significantly with decreasing layer thickness), and the decrease in aging rate for films with thinner layers was found to correlate with an increase in interphase fraction. The elevated T_g of the interphase material (compared to pure PS) was suggested as a possible reason for reduced aging rates in the thin PS layers. In the second method, PS layers were cooled from above their T_g at different rates under confinement by PC layers. After this cooling step was performed, subsequent heating thermograms revealed that the enthalpy recovered upon reheating through the T_g of PS was similar for bulk and nanolayered films.

1. Introduction

Glassy polymers are non-equilibrium materials with excess thermodynamic quantities such as specific volume, enthalpy and entropy [1,2]. The structural relaxation of glassy polymers towards a thermodynamic equilibrium state, which is accompanied by changes in many properties, is often referred to as “physical aging” [3]. Physical aging of polymers below the glass transition temperature involves densification via molecular rearrangements [1,4]. Aging affects mechanical, optical and gas transport properties (among others) [5,6], and the effects can be particularly intense and diverse when the polymer is confined on the nanoscale. Many important thin film and nanomaterial applications such as nanocomposites, microelectronics, and separation membranes utilize polymers that are confined [7–10]. It is necessary to understand the structural relaxation of glassy polymers and the effect of substrate confinement if the polymers are to be integrated effectively into modern applications.

Various techniques have been used to track physical aging in polymers. Some commonly used techniques for studying structural relaxation in thin films include differential scanning calorimetry (DSC) [11], gas permeability [12,13], fluorescence spectroscopy [14,15], reflectometry [16] and ellipsometry [17,18]. One approach that has been used to study the structural relaxation of glassy polymers involves cooling the melt at different rates and investigating the resulting physical properties [19].

Different experimental techniques and types of confinement have been employed to study T_g and aging behavior in glass-forming polymers. In studies by Koh and Simon [11] and Kim et al. [17], T_g reduction was observed with decreasing film thickness. It was shown that the depression in T_g becomes significant at thicknesses less than 100 nm. In contrast, other studies on confined films showed increases in T_g [20] and thickness-independent T_g [21]. Decreases in T_g with confinement are commonly observed when the polymer possesses at least one free surface. Free-standing thin films and some substrate-supported films (e.g., polystyrene

* Corresponding author.
E-mail address: Exb6@cwru.edu (E. Baer).

0032-3861/$ – see front matter © 2012 Elsevier Ltd. All rights reserved.
doi:10.1016/j.polymer.2012.02.044

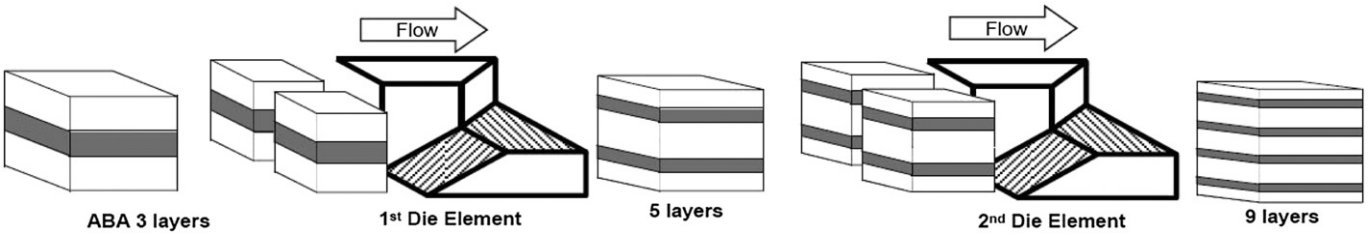

Fig. 1. Layer-multiplying coextrusion of polymer nanolayers by forced assembly. The polymer melts are combined in the ABA feedblock and split vertically at the layer-multiplying die element, then spread horizontally and recombined. The figure illustrates how two elements multiply the number of layers from 3 to 9. An assembly of n die elements produces $2^{(n+1)}+1$ layers with polymer A layers on both sides of the film. The melt is finally spread in a film die to further reduce the layer thickness.

films on silicon wafers) have been shown to have reduced T_g relative to bulk. Increases in T_g upon confinement are generally attributed to attractive polymer-substrate interactions that restrict polymer mobility near the interface, such as PMMA on silica [14]. Clearly, the T_g behavior of thin films is complex, and it remains an important area of study in the polymer literature.

Huang and Paul used gas permeability measurements to study the aging behavior of freestanding polysulfone (PSF) films ranging in thickness from 413 nm to 61 μm [13]. Decreasing gas permeability was observed with increasing aging time, as expected, since aging leads to a reduction in the free volume available for gas transport. Faster aging was observed as the film thickness was reduced. One possible explanation given for the observed behavior was an increased rate of free volume diffusion and escape at the surface of a thin film compared to a bulk film. Rowe et al. studied the aging of freestanding PSF films as thin as 20 nm in the presence of a PDMS coating layer (to eliminate pinhole defects and block convective gas transport) and found that aging persists in even the thinnest films [22]. The initial permeability of the films was found to decrease with decreasing thickness. It should be noted that the gas permeation studies of Rowe et al. and Huang et al. were conducted at temperatures well below the T_g of the materials used (~150 °C below the T_g of PSF), while many other studies were performed at aging temperatures much closer to the T_g of the polymers that were studied (typically less than 30 °C below T_g). A study by Koh and Simon found that the aging rates of stacked ultrathin PS films were reduced (compared to bulk) when aged at the same temperature [11]. Despite the fact that the aging rates (defined in their work as the slope of the linear region of a plot of fictive temperature versus log time) for ultrathin films were lower than the bulk value at a given temperature, the confined samples required less time to reach equilibrium. Thus, aging in the ultrathin films was judged to be accelerated relative to bulk. When aged at an equivalent distance from T_g (the ultrathin films have T_gs lower than the bulk value), the aging rates for bulk and ultrathin stacked films were similar. The work of Koh and Simon helps illustrate some of the complexities involved in studying physical aging in confined polymers. Priestley et al. studied the effect of substrate interaction on the aging of thin films via a technique utilizing dye-labeled polymethyl methacrylate (PMMA) films produced by spin-coating [14]. Physical aging of PMMA was studied by measuring the changes in the fluorescence intensity during aging. For a single layer PMMA film aged at a given temperature, the aging rate increased as the thickness was increased from 35 nm to 300 nm and became independent of layer thickness above 300 nm. Tri-layer PMMA films were found to undergo faster aging in the core layer as compared to surface or substrate layers. Interfacial effects were found to be significant in nanoconfined PMMA, and it was shown that the substrate–polymer interaction perturbs the relaxation of polymer. These examples show that the complex dynamics of confined glassy polymers is still not fully understood.

In this paper, we discuss an alternative type of confinement that allows for probing the size-dependent physical aging of a wide variety of melt-processable polymers. This approach involves coextrusion of two or more polymers to create multilayered films with tunable layer thicknesses. Multilayer film coextrusion offers a unique opportunity to probe the physical aging of glassy polymers under different confining substrates. Coextrusion of a model glassy polymer, polystyrene (PS), against a higher-T_g polymer, polycarbonate (PC), provides a means for investigating the physical aging of PS under a "hard" confinement by PC. The results will have important implications for understanding the behavior of confined glassy polymer structures.

2. Experimental

2.1. Materials and processing

The grade of PS used was Dow Styron 685D, which has a bulk density of 1.04 g/cm^3 (ASTM D792), M_w = 527 kg/mol, and a melt flow index (MFI) of 1.5 g/10 min (ASTM D1238). The grade of PC used was Calibre 200–10 with an MFI of 10 g/10 min (1.2 kg load at 300 °C), M_w = 29.5 kg/mol, and a density of 1.2 g/cm^3. Both polymers were obtained from The Dow Chemical Company. A series of films composed of alternating layers of PS and PC were coextruded at 260 °C using a two-component forced assembly coextrusion process described previously [23,24]. A schematic illustration of the multilayer coextrusion process is shown in Fig. 1. The films have a 50/50 PS/PC composition (by volume) and contain 513 layers. Details of film samples are reported in Table 1.The nominal thickness of the PS layer for each film sample was calculated from the composition and the overall film thickness.

2.2. Atomic force microscopy

The layer thickness of the PS/PC films was measured using atomic force microscopy (AFM), which also allows for assessment of the layer integrity and continuity. Multilayered films were embedded in beam capsules using epoxy (5 min epoxy, Devcon, Rivera Beach, FL) and cured overnight at room temperature. The

Table 1
Details of PS/PC multilayered films.

Number of layers	Total film thickness (μm)	PS or PC layer thickness (nm)
PS control	125	125 μm
512 Layers PS/PC 50/50	250	500
	150	300
	100	200
	50	100
	25	50

cross-sections of the embedded films were microtomed with an ultramicrotome (MT6000-XL from RMC, Tucson, AZ) cooled by liquid nitrogen to −60 °C. AFM images were obtained in air with a commercial scanning probe microscope (Nanoscope IIIa, Digital Instruments, Santa Barbara, CA) operated in the tapping mode. The scans were carried out at ambient conditions using a rectangular type Si probe with a spring constant of 50 $Nm^{-1}$and a resonance frequency in the range of 284–362 kHz. The tip radius was 10 nm.

2.3. Physical aging at temperatures below T_g

Isothermal physical aging of PS was carried out at 80 °C in a Perkin–Elmer Pyris differential scanning calorimeter (DSC) calibrated with indium and tin. The aging temperature chosen was well below the T_g of PS ($T_g \sim 104$ °C). An identical thermal history for all nanolayered films was ensured by performing an annealing step prior to the aging experiments. The annealing step allows one to selectively "reset" the thermal history of the PS layers while leaving the PC layers in the glassy state. The multilayered films were heated in a DSC pan to 135 °C for 15 min and quenched to room temperature at a cooling rate of 200 °C/min. Thermally reset films were then aged at 80 °C (24 °C below bulk PS T_g) for various times in the DSC, followed by subsequent heating at 20 °C/min. The resulting thermograms were analyzed to calculate the recovered enthalpy from the peak observed at the T_g. A bulk control film of pure PS was also subjected to the same thermal treatment and used for comparison to multilayered films. All calculated enthalpies were normalized per unit mass of PS.

2.4. Effect of cooling rate

The effect of cooling rate on enthalpy relaxation was also investigated using DSC. Multilayered films of PS/PC and PS control were held at 135 °C for 15 min in aluminum pans and then cooled at rates of 0.05, 0.1, 0.5, 1, 2, 5, 10, 40, and 60 °C/min to 35 °C and immediately heated to 135 °C. Subsequent heating thermograms were obtained at 20 °C/min. The heating thermograms were analyzed to calculate the enthalpy recovered upon reheating through T_g.

3. Results and discussion

3.1. Layer structure of extruded and thermally reset PS/PC films

An example AFM image of the cross-section of a multilayered PS/PC film with a target layer thickness of 100 nm is shown in Fig. 2(a). The AFM image shows good layer integrity for PS and PC layers, with a measured layer thickness of 105 ± 15 nm. To investigate the possible effects of the previously described annealing procedure on layer thickness and layer integrity, AFM images of annealed films were prepared. It is important to note that the PC layers remained in glassy state during this process; only the PS layers were equilibrated above their T_g, so layer breakup was not anticipated. The AFM cross-section image of a thermally reset PS/PC film showed that the layer integrity and layer thickness was maintained (see Fig. 2b). Visual inspection of the annealed films indicated that film clarity and transparency was not altered, which also confirmed the absence of layer break-up during thermal treatment.

3.2. Glass transition temperature of PS layers

DSC was used to investigate the effect of confinement on the T_g of PS layers. The T_gs of PS in layered confinement obtained after cooling the molten PS layers at 60 °C/min are shown in Table 2.

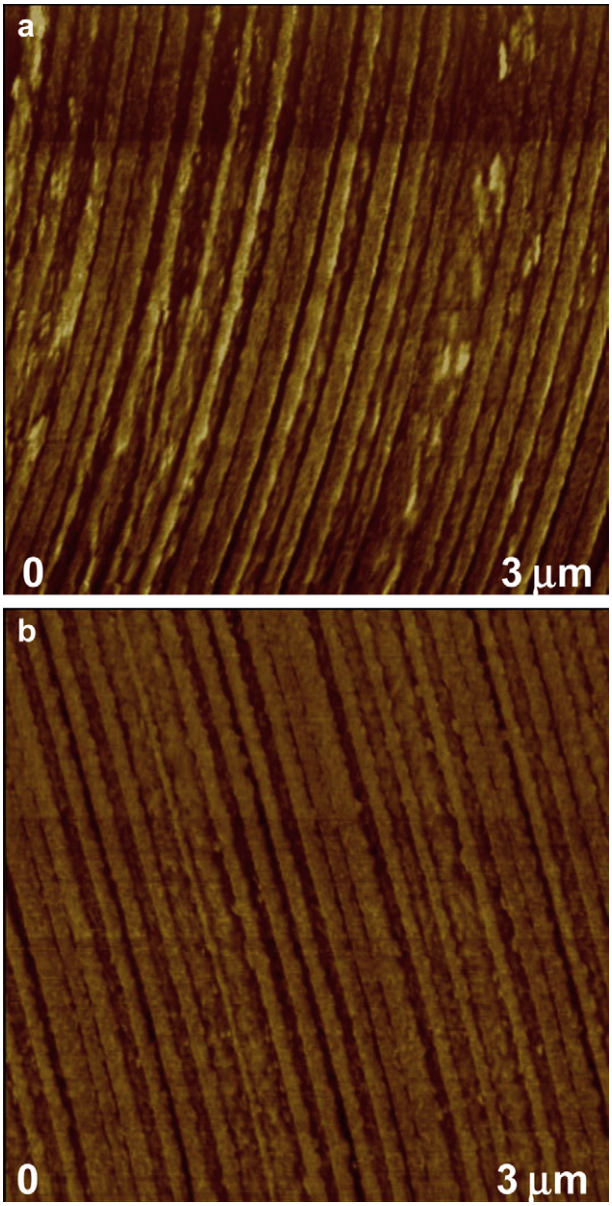

Fig. 2. AFM images of 50/50 PS/PC multilayered films. (a) As-extruded film with target layer thickness of 100 nm and measured thickness of 105 ± 15 nm. (b) Film after annealing at 135 °C for 15 min and then quenching to room temperature. The target layer thickness was 100 nm, and the measured layer thickness was 102 ± 15 nm.

Analysis of the T_g of PS layers in the multilayered films showed no systematic changes with decreasing layer thickness. This result is particularly interesting, because in many prior studies the T_g of thin glassy polymers was strongly dependent on thickness and substrate interaction. For example, Koh and Simon observed that

Table 2
T_g of PS layers obtained by DSC after cooling at 60 °C/min.

PS thickness (nm)	T_g (°C)
125 μm	104.0
500	103.4
300	103.4
200	104.9
100	104.1
50	103.7

the T_g of stacked ultrathin PS films decreased from 103 to 92 °C when the film thickness changed from a few microns to 38 nm [11]. In contrast to the work of Koh and Simon, several studies have also reported thickness-independent T_g in freestanding and supported thin films [21,25]. In the current work, the confined PS layers have a relatively weak interaction with the PC substrate; however, there is some interpenetration of PS and PC segments at the interface on a scale of the order of ~3 nm. Confinement of polymers by inorganic substrates generally does not permit such interpenetration. The interpenetration at the interface is discussed in greater detail later in this paper and has important implications in designing nanoconfined systems.

3.3. Aging of PS layers below T_g

Aging of thermally reset multilayered films was performed at 80 °C, which is well below the PS T_g of 104 °C. Heating thermograms for the films aged at various times were recorded using DSC. Thermograms for 125 μm bulk PS control films and PS/PC films with 50 nm PS layers are shown in Fig. 3. An increase in heat capacity overshoot at T_g with increasing aging time was observed in all the film samples. A graphical example of the method used to calculate the recovered enthalpy (ΔH) of a PS control film that was aged for 20 h is shown in Fig. 4. The recovered enthalpy was calculated by subtracting a reference DSC thermogram (a film sample aged for 10 min) from the thermogram for an aged sample and then using the DSC software to integrate the resultant curve according to Eq. (1) below (the DSC software accounts for the heating rate of the temperature scan when integrating the curve).

$$\Delta H = \int_{T_1}^{T_2} \left[C_p^{aged}(T) - C_p^{ref}(T) \right] dT \tag{1}$$

T_1 and T_2 represent temperatures below and above the T_g, respectively (see Fig. 4). This approach has been commonly used in previous DSC aging studies [26]. The calculated recovered enthalpy values were plotted as a function of aging time in Fig. 5. A monotonic increase in the recovered enthalpy with increasing aging time

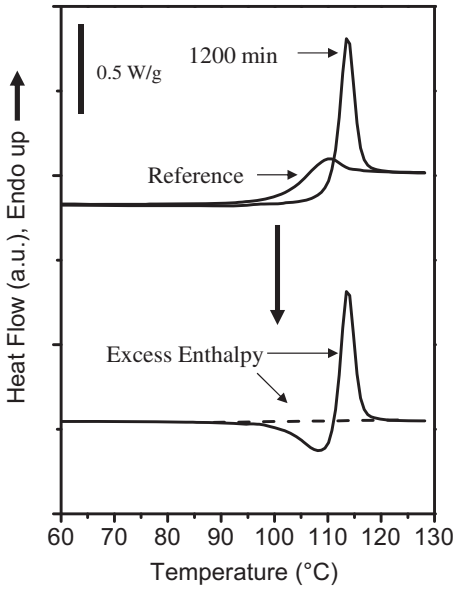

Fig. 4. Procedure for calculating the enthalpy recovered upon heating through T_g. An example of a PS control film aged for 1200 min and a reference thermogram obtained after aging the film for 10 min are shown. The reference thermogram was subtracted from the thermogram of the aged sample to obtain the lower curve, which can be integrated from T_1 to T_2 to calculate the recovered enthalpy (see Eq. (1)). The patterned sections indicate the area obtained upon integrating, and the dashed line shows the horizontal baseline spanning from T_1 to T_2 (values below this line are negative).

was observed for both control and nanolayered PS films. The PS control film showed consistently higher enthalpies at a given aging time than the PS layers under confinement. The calculated enthalpy increase was approximately linear with respect to logarithmic time. For this type of study, an aging rate can be defined as,

$$r = \frac{d(\Delta H)}{d(\ln t)} \tag{2}$$

where ΔH represents the enthalpy recovered during heating (in units of J/g). Aging rates calculated from the data shown in Fig. 5 are reported in Table 3. The aging rate for a bulk PS sample was 0.45,

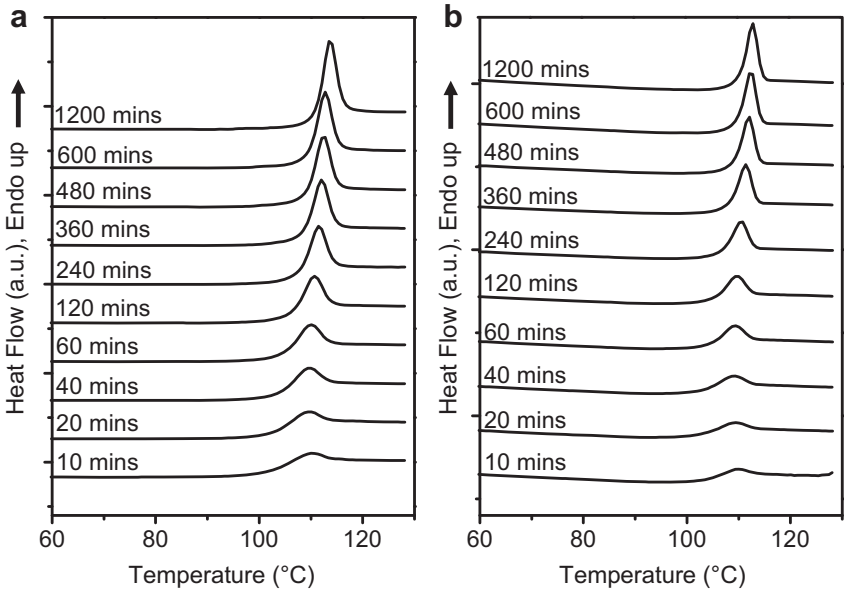

Fig. 3. DSC thermograms of (a) 125 μm PS control films (b) 50 nm PS layers, obtained at 20 °C/min after aging the film samples at 80 °C. The aging times are as indicated on the thermograms.

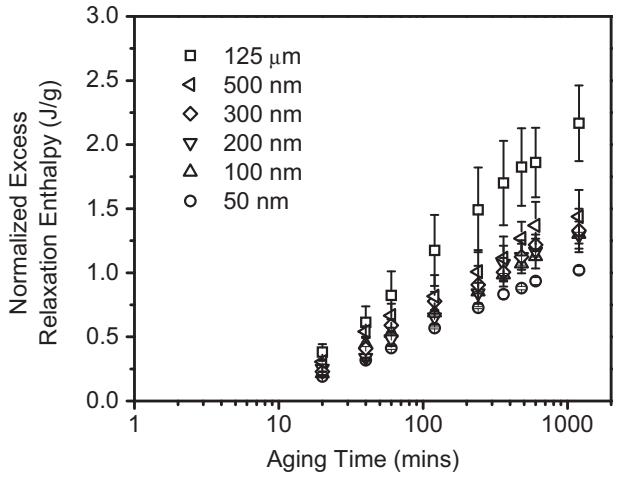

Fig. 5. Recovered enthalpy calculated after aging the films at 80 °C for various times. The calculated enthalpies were normalized for composition.

whereas the aging rate was 0.37 for a film with 500 nm PS layers. Films with 50 nm layers showed an even slower aging rate of 0.22, which was approximately 50% lower than the aging rate of the bulk PS control film. Previous studies of freestanding ultrathin films have reported faster aging rates with decreasing film thickness [2,27,28]. The accelerated aging observed in such thin films was attributed to either (a) the increased proportion of polymer chains near a highly-mobile free surface for thin films compared to bulk [22] or (b) free volume diffusion to the surface [27,28]. It was suggested that the rate of diffusion of free volume of polymer to the surface was dependent on the film thickness. As the films thickness is decreased, the timescale for free volume diffusion decreases, resulting in faster aging of thin films. In contrast to the freestanding thin films used in the above studies, the current multilayered films consisted of PS layers confined by PC. The polymer–polymer interfaces created via coextrusion eliminated the free surfaces associated with thin freestanding films for all PS layers except those at the film surface. It can be argued that the diffusion and elimination of free volume in the PS layers could be inhibited by the confining PC layers. Additionally, PS chain mobility in the layered films could also be restricted due to mechanical constraints imposed by the PC layers. It was reported previously that the polymer–substrate interaction can play an important role in the aging of ultrathin films. For example, 20 nm PMMA films on a silica substrate exhibited slower aging than 500 nm films at various temperatures [14]. In our case, interaction of PS with the confining PC layers could also have significant effects on the aging rate.

3.4. Effect of interphase on physical aging

During extrusion, some degree of mixing will take place at the interface of the PS and PC layers. An interphase region containing a blend of the two components will be formed, the thickness of which is determined by the interaction between the two polymers. Two approaches based on the theoretical work of Helfand and Tagami [31,32] were taken to estimate the interfacial thickness (d_I). The first involves the use of binary interaction energies obtained from analysis of experimental blend phase behavior, a method employed by Merfeld et al. [29] in studying the interfacial thickness and interfacial energy of polymer bilayers. Merfeld used the following equation from the Helfand–Tagami theory to calculate the interfacial thicknesses of different polymer pairs.

$$d_I = \sqrt{\frac{2RT}{B}}\left(\beta_A^2 + \beta_B^2\right)^{1/2} \tag{3}$$

B is the binary interaction energy density for the polymer pair (A and B), and β is a parameter related to the dimensions of the polymer coil. Their work notes excellent agreement between the experimental interphase thickness from neutron reflectivity measurement and the calculated value from Helfand–Tagami theory for a bilayer film of PC and a styrene-acrylonitrile copolymer (25 wt. % acrylonitrile). The second approach uses solubility parameters and a reference molar volume to estimate the interaction parameter, χ, which then can be used to determine the interphase thickness, d_I, from the following version of the Helfand-Tagami theory:

$$d_I = \frac{2b}{(6\chi)^{1/2}} \tag{4}$$

where b is the statistical segment step length, usually taken as 6 Å [32]. This correlation was successfully used to describe the interphase thickness resulting from forced assembly coextrusion of glassy polymers [30]. The method using experimental binary interaction energies makes fewer assumptions and avoids the use of any arbitrary reference volume. For the system of PC and pure PS, Merfeld et al. calculated an interphase thickness of 3.46 nm using the binary interaction energies reported in their work [29]. The interaction parameter used in the second method was obtained using the following equation:

$$\chi = \frac{V}{RT}(\delta_{PC} - \delta_{PS})^2 \tag{5}$$

Table 3
Aging rates calculated from Eq. (1) for PS layers aged isothermally at 80 °C.

PS thickness (nm)	Aging rate
125 μm	0.45
500	0.37
300	0.30
200	0.29
100	0.26
50	0.22

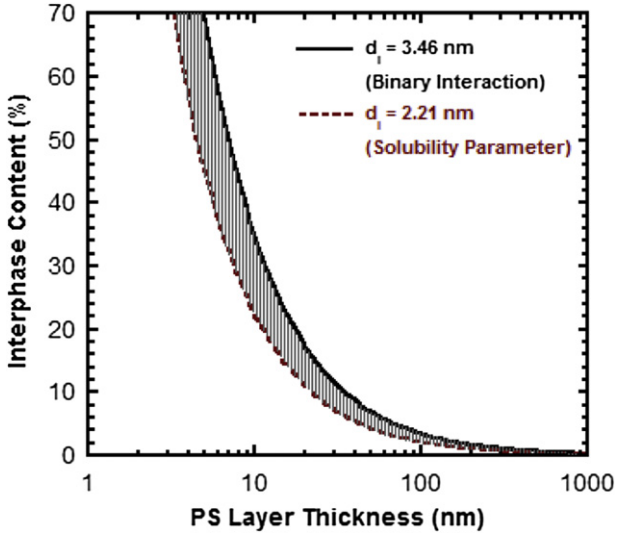

Fig. 6. Estimated interphase content in PS layers calculated using Eq. (4). Interphase thickness was calculated using value from Merfeld et al. [29] and solubility parameter method (Eq. (3)).

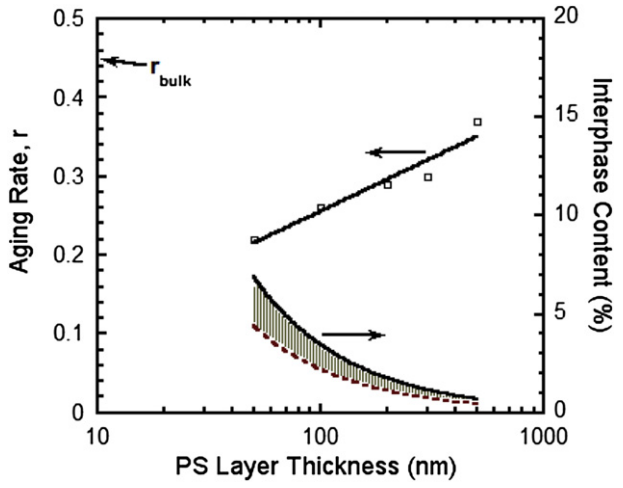

Fig. 7. Relationship between the estimated interphase fraction in PS layer for PS/PC films and the isothermal aging rates of the PS layers at 80 °C. The bulk aging rate (r_{bulk}) shown was calculated from aging data for a 125 μm bulk PS film (see Fig. 5 for bulk aging data).

where δ_{PC} and δ_{PS} are the solubility parameters for PC and PS, V is the reference molar volume (taken as the arithmetic average of the molar volumes of the PC and PS repeat units), R is the universal gas constant, and T is the processing temperature of 260 °C. Using the values of $\delta_{PC} = 9.58$ $(cal/cm^3)^{1/2}$ and $\delta_{PS} = 9.0$ $(cal/cm^3)^{1/2}$, $\chi = 0.049$ was obtained [34]. The χ parameter was used to estimate the interphase thickness in order to investigate the possible effect of interphase fraction on the physical aging of PS layers under confinement. Prior work on a variety of other multilayered films showed strong correlation between experimental and calculated values of interphase thickness using this method [34]. A quantitative relationship between the interaction parameter, χ, and the interphase composition was obtained by Helfand and co-workers [31–33]. Using the interaction parameter for PC and PS as calculated earlier using Eq. (5), the interphase thickness was calculated to be 2.21 nm. In previous work, merging of the T_gs of the polymers was reported as the interphase fraction became dominant. It was particularly evident in polymers with strong interactions. In some cases, the T_g of the interphase material was higher than that of either homopolymer [34]. For a PS layer of thickness l_{PS} that is sandwiched between PC layers, the volume fraction of interphase material (φ_I) in the PS layer can be calculated using the equation below:

$$\varphi_I = \frac{d_I}{l_{PS}} \tag{6}$$

Theoretical curves based on Eq. (6) are shown in Fig. 6. The interphase fraction increases rapidly with decreasing layer thickness.

A plot comparing the aging rate and interphase fraction as a function of PS layer thickness is shown in Fig. 7. The plot appears to indicate that the aging rate and interphase fraction may be related. For the samples with 50 nm layers, the interphase content is the highest among the films studied (4.4%–6.9%, depending on the method used), while the aging rate is the lowest. A significant decrease in the specific volume and free volume hole size of the resulting interphase material (indicating densification) was observed in previous work [31]. It was observed that the rate of enthalpy relaxation in PS was reduced as the interphase fraction increased. One possible reason for this is that the increased T_g in the interphase material (and thus greater magnitude of $T_g - T_a$) results in longer relaxation times and slower aging. The higher-T_g interphase material could also impose a mechanical constraint on relaxation in the PS layers that becomes more significant as the interphase content increases. It is speculated that the aging rate will be attenuated when the confining polymers have strong interaction and/or high interphase fraction.

3.5. Effect of cooling rate on structural relaxation of PS

Another approach for investigating the structural relaxation of PS nanolayers under confinement involves cooling the films into the glassy state (from the annealing temperature of 135 °C) at different rates. Subsequent heating thermograms were obtained at

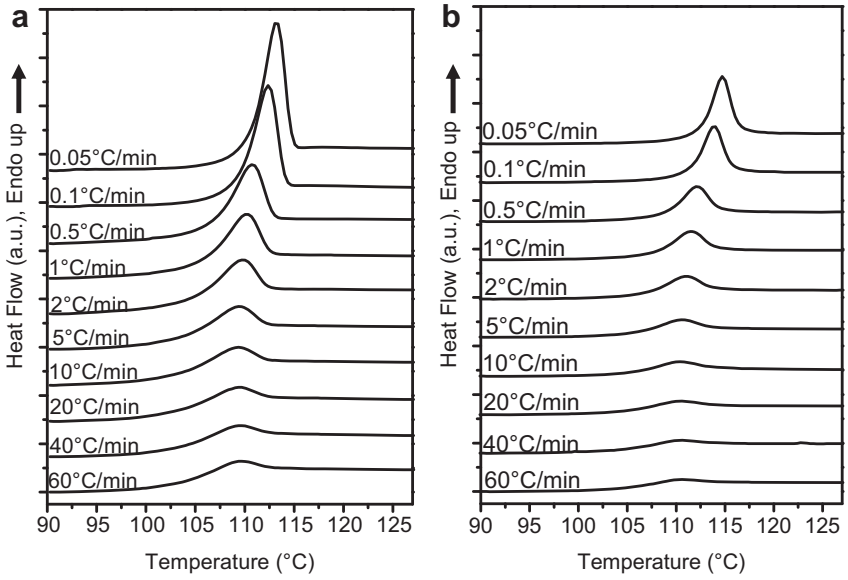

Fig. 8. DSC thermograms of (a) 125 μm PS control films (b) 50 nm PS layers obtained at 20 °C/min after cooling from the melt at different rates. The cooling rates are indicated on the thermograms.

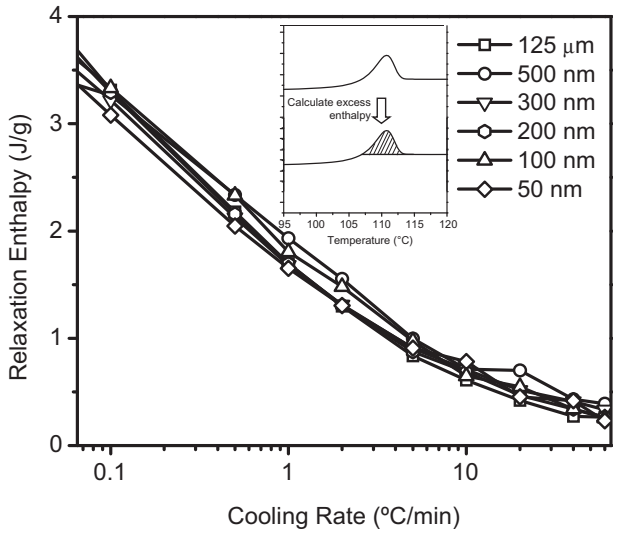

Fig. 9. Recovered enthalpy calculated after cooling PS melts at different rates. The calculated enthalpies are normalized for composition. The relaxation enthalpy was calculated as shown in the inset.

a constant heating rate of 20 °C/min. It is important to note that the samples were reheated immediately after quenching, so the reheating scans essentially capture only the relaxations that occur during the previous cooling step rather than any relaxations that occur due to isothermal aging. Two examples (a 125 μm PS control and a multilayered film with 50 nm PS layers) are shown in Fig. 8. Both examples showed an increase in the magnitude of the enthalpy overshoot with decreasing cooling rate, as expected. The structural relaxation of PS chains during slow cooling results in lower excess free volume, as slow cooling permits a greater degree of structural relaxation in the near-T_g regime. Faster cooling resulted in less stabilized glasses, while decreasing cooling rates formed increasingly stabilized glasses. The calculated ΔH values for various film samples cooled at different rates are shown in Fig. 9, along with the method of calculation for ΔH (see inset). The results imply that the relaxation of PS when cooled from above T_g at various rates is not a function of PS layer thickness (down to 50 nm) and is unaffected by the presence of adjacent PC layers.

4. Conclusions

The physical aging of confined PS layers in PS/PC films produced via multilayer coextrusion was successfully investigated using DSC. The layer integrity and layer thicknesses in extruded and thermally reset multilayered films were confirmed by AFM. Two approaches were used to study the structural relaxation of PS in this type of confinement. Isothermal aging of thermally reset PS/PC films was carried out at 80 °C to study the effect of layer thickness on physical aging, and it was observed that the aging rate was dependent on the PS layer thickness. A significant reduction in the aging rate was observed when the PS layer thickness decreased from 500 to 50 nm. It was suggested that the increased interphase fraction with decreasing layer thickness could impact the aging behavior of PS. Another approach, in which the PS/PC films were cooled at different rates, was also employed to probe the relaxation of confined PS layers. The subsequent heating thermograms of PS/PC films obtained after cooling PS at different rates revealed that the relaxation behavior of PS layers appeared to be unaffected by the presence of adjacent PC layers. It was observed that the structural relaxation of PS upon cooling from the melt was similar to bulk PS films, which is significantly different than what was observed during isothermal aging in the glassy state.

Acknowledgements

Financial support from the NSF Science and Technology Center for Layered Polymeric Systems (Grant 0423914) is gratefully acknowledged.

References

[1] Struik LCE. Physical aging in amorphous polymers and other materials. Amsterdam: Elsevier; 1978.
[2] Pfromm PH, Koros WJ. Polymer 1995;36:2379–87.
[3] Hutchinson JM. Prog.Polym Sci 1995;20:703–60.
[4] Hodge IM. Science 1995;267:1945–7.
[5] Kim JH, Koros WJ, Paul DR. Polymer 2006;47:3094–103.
[6] Kim JH, Jang J, Lee DY, Paul DR. Macromolecules 2002;35:311–3.
[7] Baker RW. Membrane technology and applications. 2nd ed. Wiley; 2004.
[8] Frank CW, Rao V, Despotopoulou MM, Pease RFW, Hinsberg WD, Miller RD, et al. Science 1996;273(5277):912–5.
[9] Reiter G, Botiz I, Graveleau L, Grozev N, Albrecht K, Mourran A, et al. Lect Notes Phys 2007;714:179–200.
[10] Mcculloch I. Nat Mater 2005;4:583–4.
[11] Koh YP, Simon SL. J Polym Sci Part B Polym Phys 2008;46:2741–53.
[12] Huang Y, Paul DR. Polymer 2004;45:8377–93.
[13] Huang Y, Paul DR. Macromolecules 2005;38:10148–54.
[14] Priestley RD, Ellison CJ, Broadbelt LJ, Torkelson JM. Science 2005;309:456–9.
[15] Ellison CJ, Kim SD, Hall DB, Torkelson JM. Eur Phys J E 2002;8:155–66.
[16] Robertson CG, Wilkes GL. Polymer 1998;39:2129–33.
[17] Kim JH, Koros WJ, Paul DR. J Membr Sci 2006;282:21–31.
[18] Baker EA, Rittigstein P, Torkelson JM, Roth CB. J Polym Sci Part B Polym Phys 2009;47:2509–19.
[19] Hadac J, Slobodian P, Riha P, Saha P, Rychwalski RW, Emri I, et al. J Non-Cryst Solids 2007;353:2681–91.
[20] Keddie JL, Jones RAL, Cory RA. Faraday Discuss 1994;98:219–30.
[21] Efremov MY, Warren JT, Olson EA, Zhang M, Kwan AT, Allen LH. Macromolecules 2002;35:1481–3.
[22] Rowe BW, Freeman BD, Paul DR. Polymer 2009;50:5565–75.
[23] Mueller CD, Kerns J, Ebeling T, Nazarenko S, Hiltner A, Baer E. In: Coates PD, editor. Polymer process engineering. Cambridge: University Press; 1997.
[24] Mueller CD, Nazarenko S, Ebeling T, Schuman TL, Hiltner A, Baer E. J Appl Polym Sci 1997;37:355–62.
[25] Pu Y, White H, Rafailovich MH, Sokolov J, Patel A, White C, et al. Macromolecules 2001;34:8518–22.
[26] Rault J. J Phys. Condens Matter 2003;15:S1193–213.
[27] McCaig MS, Paul DR. Polymer 2000;41:629–37.
[28] McCaig MS, Paul DR, Barlow JW. Polymer 2000;41:639–48.
[29] Merfeld GD, Karim A, Majumdar B, Satija SK, Paul DR. J Polym Sci Part B Polym Phys 1998;38:3115–25.
[30] Liu RYF, Bernal-Lara TE, Hiltner A, Baer E. Macromolecules 2004;37(18):6972–9.
[31] Helfand E, Tagami Y. J. Polym.Sci. Polym. Lett 1971;9:741–6.
[32] Helfand E, Tagami Y. J Chem Phys 1972;56:3592–601.
[33] Helfand E, Sapse AM. J Chem Phys 1975;62:1327–31.
[34] Liu RYF, Bernal-Lara TE, Hiltner A, Baer E. Macromolecules 2005;38:4819–27.